Current Biology, Vol. 12, 2042–2047, December 10, 2002, ©2002 Elsevier Science Ltd. All rights reserved. PII S0960-9822(02)01354-4

Motion Adaptation Distorts Perceived Visual Position

Paul V. McGraw,[1,3] David Whitaker,[1] Jennifer Skillen,[1] and Susana T.L. Chung[2]
[1]Department of Optometry
University of Bradford
Richmond Road
Bradford BD7 1DP
West Yorkshire
United Kingdom
[2]College of Optometry
University of Houston
505 J. Davis Armistead Building
Houston, Texas 77204

Summary

After an observer adapts to a moving stimulus, texture within a stationary stimulus is perceived to drift in the opposite direction—the traditional motion aftereffect (MAE). It has recently been shown that the perceived position of objects can be markedly influenced by motion adaptation [1, 2]. In the present study, we examine the selectivity of positional shifts resulting from motion adaptation to stimulus attributes such as velocity, relative contrast, and relative spatial frequency. In addition, we ask whether spatial position can be modified in the absence of perceived motion. Results show that when adapting and test stimuli have collinear carrier gratings, the global position of the object shows a substantial shift in the direction of the illusory motion. When the carrier gratings of the adapting and test stimuli are orthogonal (a configuration in which no MAE is experienced), a global positional shift of similar magnitude is found. The illusory positional shift was found to be immune to changes in spatial frequency and to contrast between adapting and test stimuli—manipulations that dramatically reduce the magnitude of the traditional MAE. The lack of sensitivity for stimulus characteristics other than direction of motion suggests that a specialized population of cortical neurones, which are insensitive to changes in a number of rudimentary visual attributes [3], may modulate positional representation in lower cortical areas.

Results and Discussion

Prolonged inspection of motion in a particular direction results in a phenomenon known as the motion-aftereffect (MAE), whereby subsequently viewed objects appear to drift in the opposite direction to that of the adapting stimulus. It has recently been suggested that this aftereffect can produce marked shifts in perceived spatial position [1, 2]. In this study we investigate the spatial selectivity of motion-induced positional shifts by introducing relative differences between the adapting and test stimuli along the dimensions of orientation, spatial frequency, and contrast. A schematic representation of the adapting and test procedure is shown in Figure 1. The stimulus elements (Gabor patches) consisted of Gaussian-windowed (envelope) sinusoidal-luminance modulations (carrier), presented in a two-blob vernier alignment test. Prior to the test phase, subjects adapted to an arrangement of stationary Gabor stimuli in which the carrier gratings drifted in opposite directions. The elements of the adapting stimulus were spatially coincident with the test elements in the two-blob alignment task. After adaptation, an illusory misalignment of the elements of the test stimulus was perceived, and the magnitude of this perceived offset was established via a method of constant stimuli.

Both the traditional MAE and the motion-induced positional offsets we describe are dependent on the drift velocity of the adapting stimulus [4]. When the carrier grating is stationary, no illusory shifts in position are observed, and the test stimulus appears aligned. Figure 2 shows that as carrier drift velocity is increased, the magnitude of the illusory positional offset also increases until it reaches a plateau (approximately 7.5 arcmin for P.V.M.; 6.5 arcmin for J.S.). Critically, the size of the positional shift is similar when the carrier grating of the adapting and test stimuli are either parallel (filled symbols) or orthogonal (open symbols) in orientation, indicating that the positional shift is independent of the orientation of the carrier grating. This demonstrates that the perception of motion per se is not important in generating the positional aftereffects because orthogonally oriented adapting and test stimuli do not result in a perceived motion aftereffect.

Many visual aftereffects show spatial tuning [4–6]. That is, the magnitude of the aftereffect is greatest when the spatial characteristics of the adapting and test stimuli match. This experimental approach has been previously employed to great effect in vision science. Seminal pattern-selective adaptation studies (both human psychophysical experiments and neurophysiological investigations in animals) reveal that early levels of the visual cortex contain independent neural mechanisms selective to stimulus' spatial characteristics, such as its orientation and spatial frequency [5, 7–9]. In order to investigate the spatial frequency-tuning characteristics of motion-induced positional shifts, we introduced a difference in carrier spatial frequency between adapting and test stimuli. This frequency asymmetry was introduced in both directions, i.e., a higher adapting carrier frequency was coupled with a lower test carrier frequency, and vice versa. In marked contrast to many previous studies examining frequency-selective adaptation [10], our study showed that the introduction of a difference, of up to two octaves, in carrier spatial frequency between the adapting and test stimuli did not significantly diminish the magnitude of the perceived shift (see Figure 3). Indeed, even when the carrier frequency of the test stimulus is reduced to zero (Gaussian blob), perceived shifts of similar size were found (PVM; 7.19 ± 0.44 arcmin, JS; 6.96 ± 0.48 arcmin). This indi-

[3]Correspondence: p.v.mcgraw@bradford.ac.uk

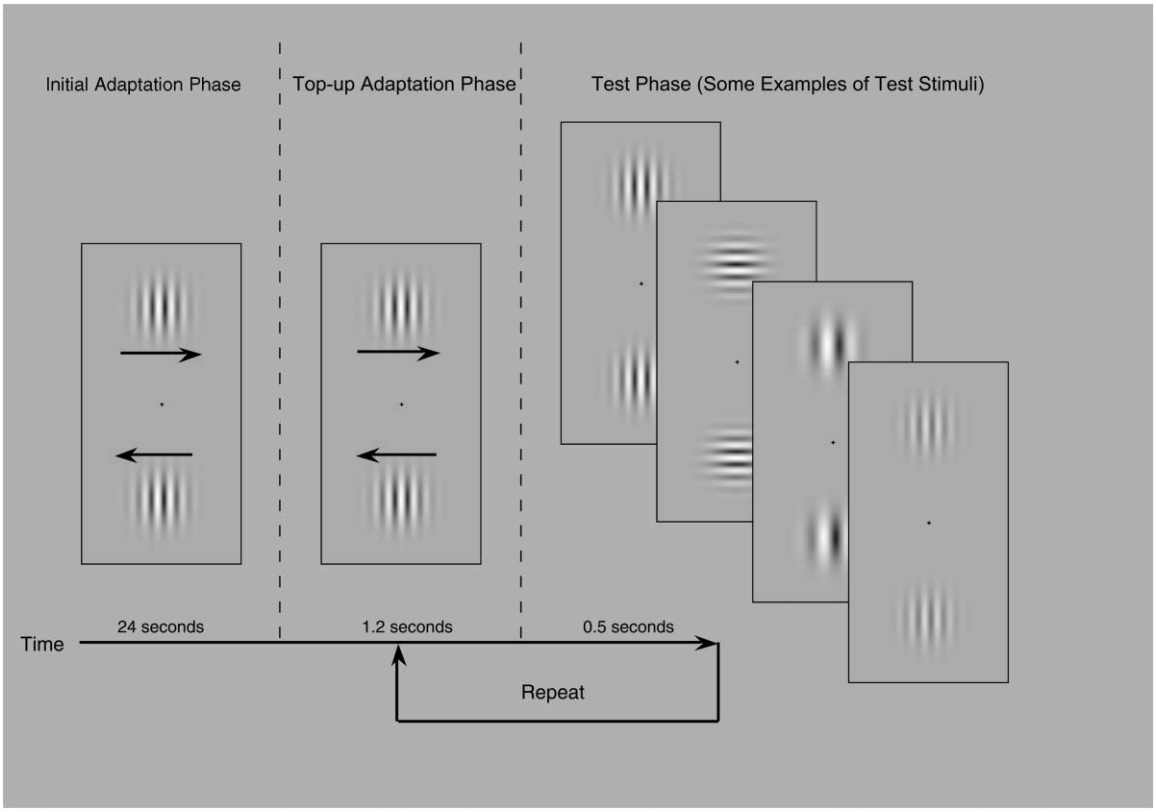

Figure 1. Schematic Representation of the Adaptation and Test Phases of the Experiment

The luminance profile of the stimuli is given by

$$L(x,y,t) = L + LC\sin[2\pi(f_s x + f_t t)]\exp^{\frac{-(x^2+y^2)}{2\sigma^2}}$$

where x and y are the horizontal and vertical distances from the center of each element, t is time, and C is the contrast modulation around a mean luminance L. The size of the elements is defined by the standard deviation, σ, of the Gaussian window. This was maintained at 0.32°. The center-to-center spacing of the two elements was 3.8°. The spatial frequency (f_x) of the carrier modulation was 4 cycles/deg, unless stated otherwise. Various carrier drift velocities were produced by changing the temporal frequency (f_t). Prior to the test phase, subjects underwent an initial period of adaptation (24 s). During this time, and throughout the experiment, fixation was held constant on a fixation mark midway between the two elements. After this initial period of adaptation, the adapting stimulus was presented for a period of 1.2 s, followed by the test phase. This cycle of top-up adaptation followed by the test phase was repeated until all trials were completed. The elements of the adapting stimulus were spatially coincident with the test elements in the two-blob alignment task. After adaptation, an illusory misalignment of the elements of the test stimulus was perceived, and the magnitude of this perceived offset was established via standard psychophysical procedures. For one experiment, we used a dichoptic arrangement in which the adapting or test stimuli could be presented on one of two monitors, which were viewed via adjustable front surface mirrors. The linearized luminance response of both monitors was matched in this set-up.

cates that, unlike many other visual aftereffects, this effect shows little if any spatial frequency tuning. This finding does, however, have parallels with studies such as stereopsis judgements and measures of positional accuracy, which do not involve a process of adaptation and for which performance can be largely independent of carrier spatial frequency [11, 12].

In addition to spatial frequency tuning, it is well established that many visual aftereffects are also sensitive to contrast differences between the adapting and test stimuli. In general, aftereffects are greatest in magnitude when the adapting stimulus has high contrast and the test stimulus has low contrast. This is certainly true in the case of the MAE [13]. The magnitude of the MAE, measured in terms of the duration of illusory motion, increases with increasing adapting contrast. Furthermore, if adapting contrast is fixed, increases in test contrast result in a reduction in the magnitude of the MAE [13, 14]. The contrast dependence of motion-induced positional shifts is shown in Figure 4. In a manner similar to their spatial frequency tuning, these positional offsets are relatively immune to changes in contrast of either the adapting or test stimuli. Despite a 16-fold change in adapting contrast relative to test contrast, in either direction, positional offsets remain relatively unchanged.

It is clear that the positional shifts resulting from motion adaptation display characteristics that are very different from those of the traditional MAE. Whereas the MAE is spatially tuned for a number of basic visual properties such as orientation, spatial frequency, and contrast, our positional shifts remain relatively constant despite the introduction of marked differences between

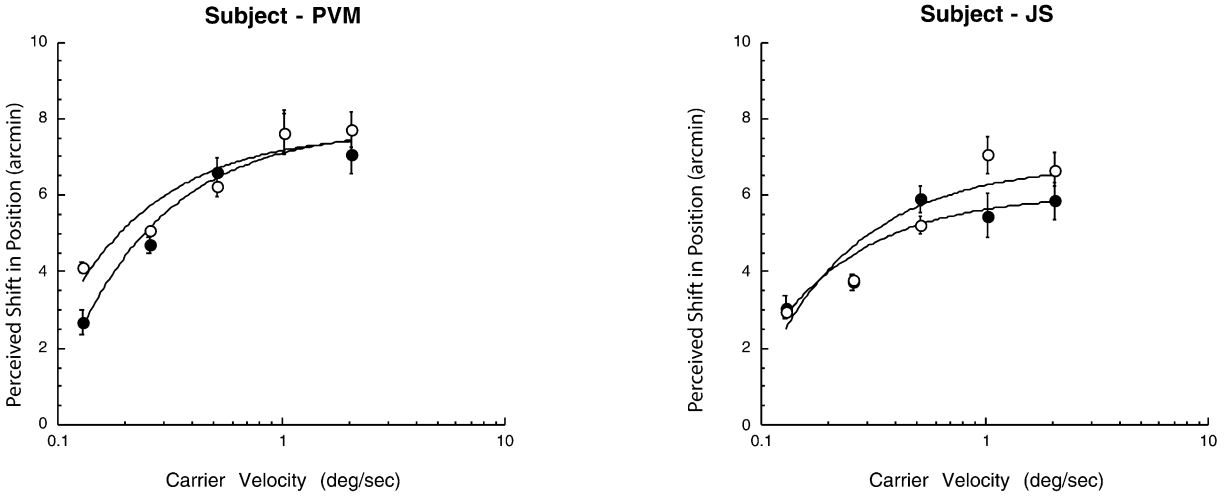

Figure 2. The Velocity Tuning of Motion-Induced Positional Shifts

Shifts of similar magnitude are found regardless of the orientation of the test stimulus relative to the adapting stimulus. Filled symbols represent the situation in which the carrier orientations are parallel in adapting and test stimuli, whereas open symbols represent orthogonally oriented adapting and test carriers.

adapting and test stimuli along each of these dimensions. So how might we reconcile these differences in response to spatial manipulations of the stimulus? One possibility is that motion-induced positional shifts are mediated by a different type of motion aftereffect. The proposition that different kinds of motion aftereffect exist is not a new one. Favreau [15] described at least two types of MAE: one that was broadly tuned for spatial parameters, dissipated quickly, and could be transferred between the two eyes and another that showed narrow spatial tuning, was more enduring, and showed little interocular transfer. Therefore, we decided to investigate the role of binocularly driven neurones in our motion-induced positional offsets. We repeated our experiment by using a dichoptic arrangement, i.e., we presented the adapting stimulus to one eye and the test stimulus to the other. The data are shown in Figure 5.

The high degree of interocular transfer of these illusory positional shifts indicates that the interaction between position and motion mechanisms occurs after binocular integration of the inputs from each eye. Favreau [15] proposed the superior colliculus as a possible locus for

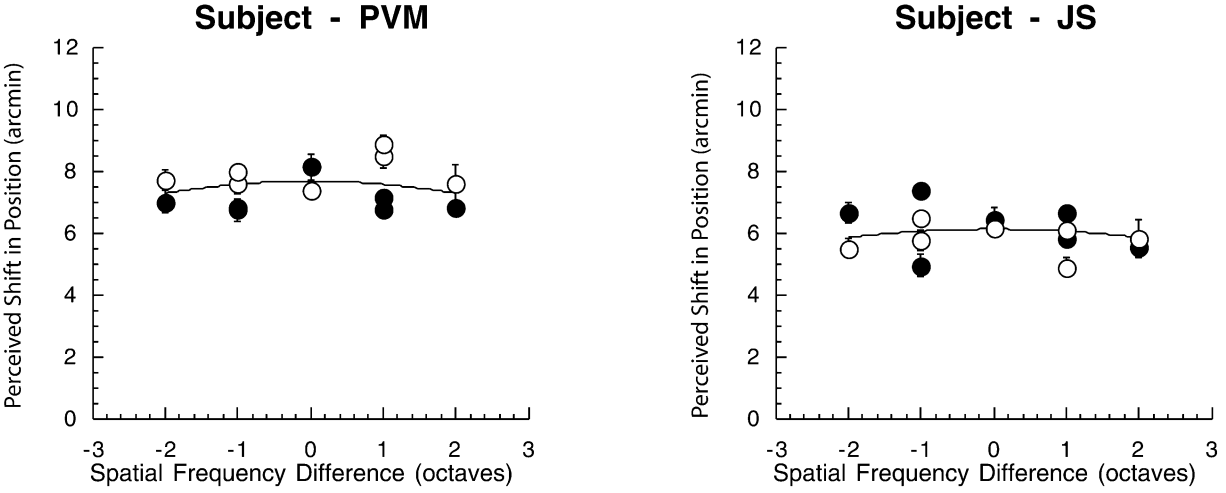

Figure 3. Lack of Spatial-Frequency Tuning of Motion-Induced Positional Shifts for Two Subjects

The spatial-frequency range of adapting and test stimuli was 1–16 cycles/deg, with a midpoint of 4 cycles/deg. The filled symbols represent the condition in which the orientation of the test carrier was parallel to that of the adapting carrier, whereas the open symbols represent orthogonally oriented adapting and test carriers. Once again, the magnitude of the perceived shifts in spatial position for parallel and orthogonally oriented adapting and test carriers are very similar, indicating almost complete crossover of the adaptation effect across orientation. Furthermore, the magnitude of the positional shifts shows little tuning for adapting or test carrier spatial frequency. The data for both conditions (parallel adapting and test carriers and orthogonal adapting and test carriers) have been fitted with a single Gaussian function. Estimates of spatial frequency bandwidths at half height were extremely broad for both subjects (P.V.M., 8.82 octaves; J.S., 9.50 octaves).

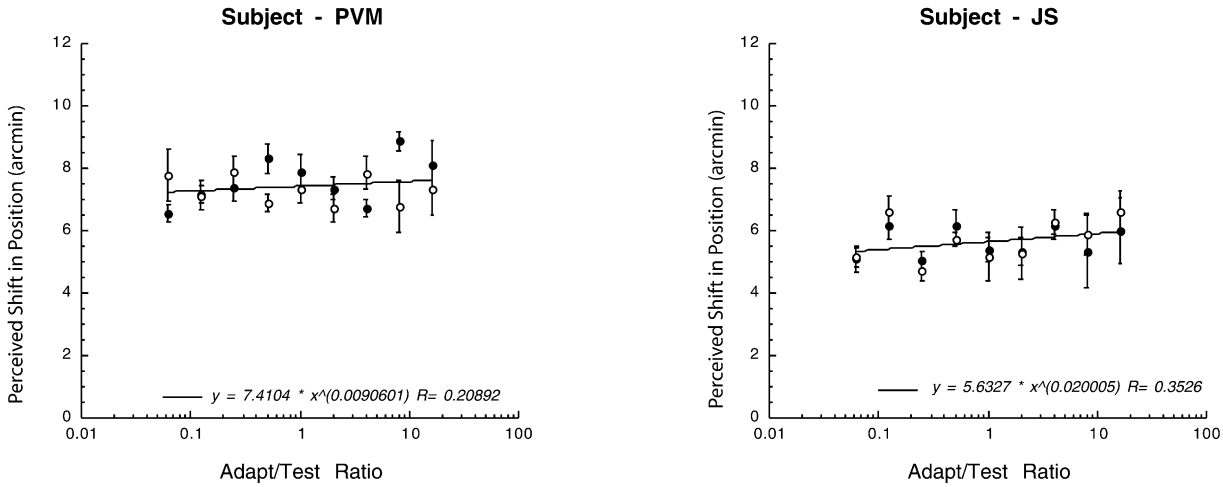

Figure 4. Contrast Dependence of Motion-Induced Positional Shifts

Despite marked changes in the contrast of the adapting stimulus relative to that of the test, and vice versa, the magnitude of perceived positional offsets shows little change. The filled symbols represent parallel adapting and test stimuli, whereas the open symbols represent orthogonal adapting and test stimuli. Each data point represents the mean positional offset for a particular adapting/test ratio. Similarly, mean errors are presented at each adapting/test ratio. The data from both conditions have been fitted with a single power function.

her broadly tuned, binocular, MAE mechanism because of the poor spatial selectivity and high degree of binocularity shown by neurons in this area. However, more recent evidence from functional magnetic resonance imaging (fMRI) studies in humans [16, 17] has placed the primary site of MAE generation firmly at the level of cortical area MT (V5). Although other areas of the striate cortex also demonstrate direction-selective adaptation (e.g., V1, V2, V3, V4v, V3A), the extent is modest compared with the degree found in extra-striate areas [17]. The MAE is, by necessity, direction specific, a property shown by a particularly high proportion of neurons located in the human equivalent of cortical area MT (V5) [17]. Furthermore, cortical microstimulation of MT neurones can significantly bias perceptual judgments of motion direction, demonstrating a functional link between neural activity at the level of MT and motion direction judgments [18].

Contemporary computational models of the MAE adopt an approach based on changes in the relative responsiveness of populations of neurones tuned to different directions of motion. The most cogent model of the MAE involves at least two stages of analysis [19], where the eventual percept reflects adaptation at each stage of processing. The initial level of analysis, termed the "sensor layer," is associated with low binocularity and marked spatial selectivity, both of which are properties associated with the traditional MAE. Excitatory and inhibitory opponent processes from the "sensor layer" converge at an "integrator layer." Adaptation at the integrator level predicts high degrees of binocularity and broad tuning for a range of stimulus attributes, as a direct result of pooling sensor layer outputs regardless of the eye of origin. The perceptual manifestation of adaptation at each of these layers is likely to reflect the physiological properties of the populations of neurones that mediate them. The sensor layer is thought to reflect the adaptive behavior of V1 neurons, whereas the integrator layer is thought to be located in cortical-area MT [20]. Indeed, there exists evidence for selective adaptation at each of these levels of motion analysis [21, 22]. The physiological identity of the neural units that comprise the model's integrator layer have not yet been firmly identified. However, that is not to say that likely candidates do not exist. In monkey area MT, a population of neurones that respond to a particular direction of motion regardless of the physical properties of the object defining the motion itself has been documented [3]. This lack of specificity for the physical characteristics of an object is reflected in the results of the present study, where the magnitude of motion-induced positional shifts remains constant in the face of marked manipulation of the stimulus contrast, orientation, and spatial frequency.

The results of the present study clearly indicate that adaptation to motion can have a significant impact on the perceived location of physically stationary objects. Furthermore, this illusory shift in position occurs regardless of whether or not the observer actually perceives motion after adaptation. Adapting to motion induces a local distortion in the positional map, and this distortion subsequently affects any stimuli falling in this area. The lack of specificity for a range of stimulus attributes, along with the fact that the effect shows almost complete interocular transfer, suggests that the motion adaptation takes place at a relatively high level of motion analysis and may be mediated by motion-analyzing neurones such as those identified by Albright [3] in area MT. A possible explanation is that motion signals, generated through adaptation, are relayed via a reentrant input stream to lower cortical areas where the neural representation of spatial position resides. The accurate representation of spatial position demands the involvement of relatively small receptive fields, such as those found in areas V1 and V2. In fact, many aspects of the positional accuracy of the visual system can be adequately de-

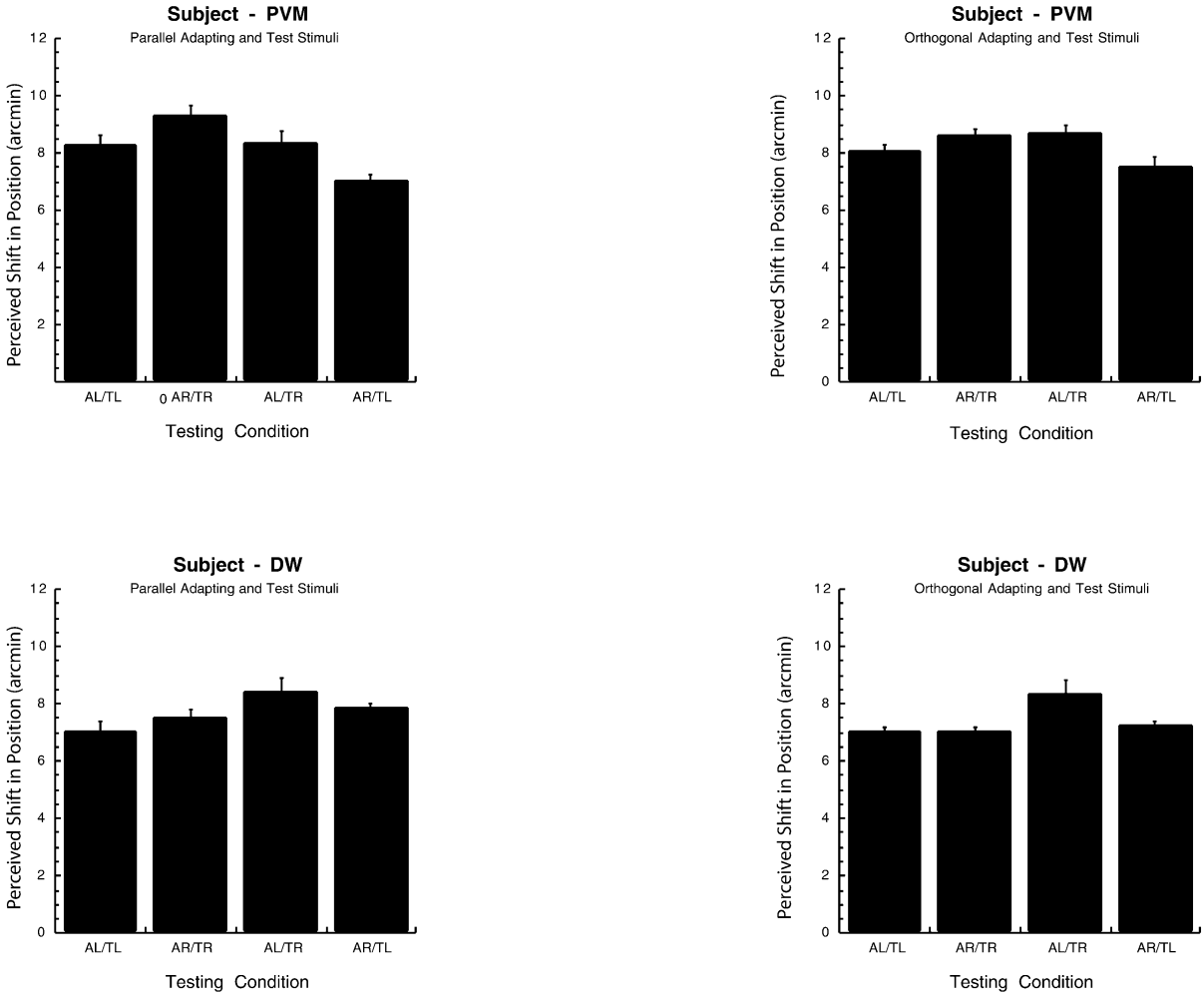

Figure 5. Interocular Transfer of Motion-Induced Positional Shifts for Each of the Four Possible Conditions

(AL/TL) adapt left, test left; (AR/TR) adapt right, test right; (AL/TR) adapt left, test right; and (AR/TL) adapt right, test left. The panels represent data for which the adapting and test stimuli were parallel (left) and for which adapting and test stimuli were orthogonal in orientation (right). There is almost complete interocular transfer of the perceived positional shifts.

scribed by models based entirely on processing at early levels of the striate cortex [23]. There are certainly established anatomical pathways connecting higher motion centers such as V5 with lower cortical areas [24]; however, their functional relevance remains a matter of conjecture. A robust test of the importance of such feedback mechanisms would be to disrupt cortical processing in area V5 immediately after motion adaptation and to examine the effect on any resultant positional shifts—this is currently the focus of work in our laboratory.

Acknowledgments

P.V.M. is supported by a Research Career Development Fellowship from the Wellcome Trust. S.C. was supported by a Travel Scholarship from the Burroughs-Wellcome Foundation.

Received: August 6, 2002
Revised: September 23, 2002
Accepted: September 23, 2002
Published: December 10, 2002

References

1. Snowden, R.J. (1998). Shifts in perceived position following adaptation to visual motion. Curr. Biol. *8*, 1343–1345.
2. Nishida, S., and Johnston, A. (1999). The influence of motion signals on the perceived position of spatial pattern. Nature *397*, 610–612.
3. Albright, T.D. (1992). Form-cue invariant motion processing in primate visual cortex. Science *255*, 1141–1143.
4. Wohlgemuth, A. (1911). On the after-effect of seen movement. Brit J Psychol Suppl *1*, 1–117.
5. Blakemore, C., and Campbell, F.W. (1969). On the existence of neurones in the human visual system selectively sensitive to the orientation of size of the retinal images. J. Physiol. *203*, 237–260.
6. Webster, M.A., and Mollon, J.D. (1991). Changes in colour appearance following post-receptoral adaptation. Nature *349*, 235–238.
7. Hubel, D.H., and Wiesel, T.N. (1968). Receptive fields and functional architecture of monkey striate cortex. J. Physiol. *195*, 215–243.
8. Campbell, F.W., Cooper, G.F., and Enroth-Cugell, C. (1969). The spatial selectivity of the visual cells of the cat. J. Physiol. *203*, 223–235.

9. Blakemore, C., Nachmias, J., and Sutton, P. (1970). The perceived spatial frequency shift: evidence for frequency-selective neurones in the human brain. J. Physiol. *210*, 727–750.
10. Cameron, E.L., Baker, C.L.J., and Boulton, J.C. (1992). Spatial frequency selective mechanisms underlying the motion aftereffect. Vision Res. *32*, 561–568.
11. Burbeck, C.A. (1987). Position and spatial-frequency in large-scale localization judgements. Vision Res. *27*, 417–427.
12. Hess, R.F., and Wilcox, L.M. (1994). Linear and nonlinear filtering in stereopsis. Vision Res. *34*, 2431–2438.
13. Keck, M.J., Palella, T.D., and Pantle, A. (1976). Motion aftereffect as a function of the contrast of sinusoidal gratings. Vision Res. *16*, 187–191.
14. Nishida, S., Ashida, H., and Sato, T. (1997). Contrast dependencies of two types of motion after-effect. Vision Res. *37*, 553–563.
15. Favreau, O.E. (1976). Motion aftereffects: evidence for parallel processing in motion perception. Vision Res. *16*, 181–186.
16. Tootell, R.B.H., Reppas, J.B., Dale, A.M., Look, R.B., Sereno, M.I., Malach, R., Brady, T.J., and Rosner, B.R. (1995). Visual motion aftereffect in human cortical area MT revealed by functional magnetic resonance imaging. Nature *375*, 139–141.
17. Huk, A.C., Ress, D., and Heeger, D.J. (2001). Neuronal basis of the motion aftereffect reconsidered. Neuron *32*, 161–172.
18. Salzman, C.D., Murasugi, C.M., Britten, K.H., and Newsome, W.T. (1992). Microstimulation in visual area MT: effects on direction discrimination performance. J. Neurosci. *12*, 2331–2355.
19. Mather, G., and Harris, J. (1998). Theoretical models of the motion aftereffect. In The Motion Aftereffect: A Modern Perspective, G. Mather, F. Verstraten, and S. Anstis, eds. (Cambridge, MA: MIT Press), pp 157–185.
20. Wilson, H.R., and Kim, J. (1994). A model for motion coherence and transparency. Vis. Neurosci. *11*, 1205–1220.
21. Verstraten, F.A.J., van der Smagt, M.J., Fredericksen, R.E., and van de Grind, W.A. (1999). Integration after adaptation to transparent motion: static and dynamic test patterns result in different aftereffect directions. Vision Res. *39*, 803–810.
22. Culham, J.C., Verstraten, F.A.J., Ashida, H., and Cavanagh, P. (2000). Independent aftereffects of attention and motion. Neuron *28*, 607–615.
23. Wilson, H.R. (1986). Responses of spatial mechanisms can explain hyperacuity. Vision Res. *26*, 453–469.
24. Shipp, S., and Zeki, S. (1989). The organisation of connections between areas V1 and V5 in the macaque monkey visual cortex. Eur. J. Neurosci. *1*, 309–322.